CCFE-PR(15)75

S. X. Yang, S. Wang, Y. Q. Liu, G. Z. Hao, Z. X. Wang, X. M. Song, and A. K. Wang

Bifurcation of resistive wall mode dynamics predicted by magnetohydrodynamic-kinetic hybrid theory

Bifurcation of resistive wall mode dynamics predicted by magnetohydrodynamic-kinetic hybrid theory

S. X. Yang,[1] S. Wang,[2] Y. Q. Liu,[3, 2] G. Z. Hao,[2] Z. X. Wang,[1] X. M. Song,[2] and A. K. Wang[2]

[1]Key Laboratory of Materials Modication by Beams of the Ministry of Education, School of Physics and Optoelectronic Technology, Dalian University of Technology, Dalian 116024, China
[2]Southwestern Institute of Physics, P.O.Box432 Chengdu 610041, China
[3]Culham Centre for Fusion Energy, Culham Science Centre, Abingdon OX14 3DB, United Kingdom

Bifurcation of resistive wall mode dynamics predicted by magnetohydrodynamic-kinetic hybrid theory

S. X. Yang,[1] S. Wang,[2] Y. Q. Liu,[3,2] G. Z. Hao,[2,*] Z. X. Wang,[1,†] X. M. Song,[2] and A. K. Wang[2]

[1]*Key Laboratory of Materials Modification by Beams of the Ministry of Education, School of Physics and Optoelectronic Technology, Dalian University of Technology, Dalian 116024, China*

[2]*Southwestern Institute of Physics, P.O.Box432 Chengdu 610041, China*

[3]*Culham Centre for Fusion Energy, Culham Science Centre, Abingdon OX14 3DB,United Kingdom*

The magnetohydrodynamic-kinetic hybrid theory has been extensively and successfully applied for interpreting experimental observations of macroscopic, low frequency instabilities, such as the resistive wall mode, in fusion plasmas. In this work, it is discovered that an analytic version of the hybrid formulation predicts a bifurcation of the mode dynamics while varying certain physical parameters of the plasma, such as the thermal particle collisionality or the ratio of the thermal ion to electron temperatures. This bifurcation can robustly occur under reasonably large parameter spaces as well as with different assumptions, for instance, on the particle collision model. Qualitatively similar bifurcation features are also observed in full toroidal computations based on a non-perturbative hybrid formulation.

PACS numbers: 52.35.Py, 52.55.Fa, 52.55.Tn

The resistive wall mode (RWM) is a low frequency, macroscopic instability driven either by the plasma current (in tokamaks or reversed field pinches) or pressure (in tokamaks) [1, 2]. Because of its global nature, the onset of this instability, or sometimes even the response of a marginally stable RWM to external three-dimensional magnetic field perturbations [3, 4], can cause major disruption in tokamaks or termination of discharges in reversed field pinch devices. This motivates extensive research that have been carried out on this instability in recent years, both in experiments [5–8] and in theory [9–16].

The mode originates from ideal external kink mode, which is a high frequency (comparable to the Alfvén frequency) instability. Whilst the kink mode is often well described by the ideal magnetohydrodynamic (MHD) theory, the RWM involves more subtle physics, essentially due to the fact that the modes frequency is much lower as a result of the surrounding wall eddy current stabilization. In fact the modes frequency, measured in the laboratory frame, is often below any of the typical drift frequencies of plasma thermal particles. Consequently, in the presence of a toroidal flow of the plasma, the mode rotates in the plasma frame. This mode rotation in the plasma frame can create resonance conditions with the particle motions, if the toroidal rotation frequency matches the toroidal precession frequency of particles, or even the bounce (transit) frequency of trapped (circulating) thermal ions. This is the primary resonance damping physics of the RWM which can be described by the drift kinetic theory [11].

The MHD-kinetic hybrid formulation, which we adopt in this work, essentially utilizes the single fluid theory to describe the mode dynamics perpendicular to the equilibrium magnetic field lines, whilst the parallel motion is kinetically treated. Neglecting the plasma inertial effect (because the mode frequency is normally small in the laboratory frame), the hybrid formulation leads to a well-known dispersion relation for the RWM [11, 17].

$$D(\omega) \equiv -i\omega\tau_w + \frac{\delta W_\infty + \delta W_k(\omega)}{\delta W_b + \delta W_k(\omega)} = 0, \qquad (1)$$

where $\omega = \omega_r + i\gamma$ is the eigenvalue (complex frequency) of the mode in the laboratory frame, with ω_r and γ being the real frequency and the growth rate, respectively. τ_w is the typical eddy current decay time of the resistive wall. For example, in a straight cylinder with circular cross section, the wall time, in response to a single m Fourier perturbation, is calculated as $\tau_w = \mu_0\sigma bd(1-a^{2m}/b^{2m})/(2m)$, with a, b, d, σ, m and μ_0 being the plasma minor radius, the wall position, the wall thickness, the wall conductivity, the poloidal mode number and the vacuum permeability, respectively. This definition of the wall time will be followed in the first part of our work, where the dispersion relation (1) is solved under simplified geometrical assumptions.

Equation (1) is equivalent to an extended energy principle for the RWM, with quantities δW_∞ and δW_b representing the perturbed fluid potential energies, without and with an ideal conducting wall, respectively. δW_k is the perturbed drift kinetic energy representing the mode-particle resonance physics. In this paper, we shall only consider the processional drift resonances of trapped thermal ions and electrons, assuming that the plasma flow (more precisely the equilibrium $\mathbf{E} \times \mathbf{B}$ flow) is slower than the thermal particle diamagnetic flow. It is important to note that we keep the mode frequency ω, though normally being small, into the mode-particle resonance condition, leading to a rather non-linear dependence of the drift kinetic energy δW_k on ω. This nonlinearity can introduce multiple branches of the RWM, as has been shown in earlier work [13, 18], and can also result in fishbone-like modes [15], if the energetic particle resonances are included. Different from early results, in this work we find that bifurcation can occur in terms of the RWM eigenvalue in the complex plane, with continuous variation of certain plasma parameters.

We adopt a model similar to that developed in Ref. [17]. Following a large aspect ratio approximation with circular plasma cross section, the perturbed drift kinetic energy can be written as [17, 19]

$$\delta W_k = 2\pi^{3/2}\sum_{e,i}\int dr\epsilon_r P C_l^2 \int d\lambda \frac{(2-\lambda)^2}{F} \times \int d\hat{\varepsilon}_k \hat{\varepsilon}_k^{5/2} e^{-\hat{\varepsilon}_k} Q, \qquad (2)$$

where $\epsilon_r = r/R_0$ is the inverse aspect ratio, $P(r) = P_0(1-r^2)$ is the equilibrium plasma pressure, which we assume to be a parabolic function of the plasma minor radius r (normalized by a), with $P_0 = \mu_0 J_0^2/4$, and J_0 being the plasma current density which is assumed to be flat along minor radius. $\lambda \equiv \mu B_0/\varepsilon_k$ is the pitch angle of (trapped) particles, μ is the magnetic moment, B_0 is the equilibrium magnetic field, $\hat{\varepsilon}_k = \varepsilon_k/T$ is the particle energy ε_k normalized by the temperature T. In this simple model, a uniform plasma equilibrium current density also yields a flat safety factor profile $q(r) = q_0 \equiv 2B_0/(\mu_0 R_0 J_0)$. The coefficient $C_{l=0} = |\langle\xi_R\rangle|$ is the plasma displacement along the major radius, averaged over one bounce period of the particle, for a single poloidal Fourier harmonic m. In particular, $\xi_R = \xi_r\cos\theta - \xi_\theta\sin\theta = (m/F_0)r^{u-1}e^{i(m-v)\theta}$, with $u = |m|$, $v = m/u$, and $F_0 = (m - nq_0)B_0/(R_0 q_0)$. n is the toroidal mode number. In a cylindrical plasma with circular cross section, C_l^2 can be analytically evaluated via $C_{l=0}^2 = (mr^{u-1}/F_0)^2 C_m^2$, where

$$C_m^2 = |\sum_{p=0}^{m-v}\begin{pmatrix} p \\ m-v\end{pmatrix}(2ik_t)^p G_p|^2. \qquad (3)$$

The above expression involves a function G_p which resembles elliptic type of integrals

$$G_p = \frac{\int_0^{\pi/2} d\varphi(1-2k_t^2\sin^2\varphi)^{m-v-p}(\sin\varphi)^p}{K(k_t^2)} \times \left(\sqrt{1-k_t^2\sin^2\varphi}\right)^{p-1}. \qquad (4)$$

Thus for the $m = 2$ perturbation, we have

$$C_{m=2}^2 = G_0^2 + 4k_t^2 G_1^2,$$

and for $m = 3$, we obtain

$$C_{m=3}^2 = (G_0 - 4k_t^2 G_2)^2 + 16k_t^2 G_1^2.$$

Here $K(k_t^2)$ is the complete elliptic integral of the first kind, and $k_t = \sqrt{(1-\lambda-\lambda\epsilon_r)/2\lambda\epsilon_r}$.

Among the remaining two factors from expression (2), $F = \pi\sqrt{2\lambda\epsilon_r}/2K(k_t^2)$ is the normalized bounce frequency, and Q is the resonance operator

$$Q = \frac{n\omega_{*N} + (\hat{\varepsilon}_k - 3/2)n\omega_{*T} + n\omega_E - \omega}{n\omega_d - i\nu_{eff} + n\omega_E - \omega}, \qquad (5)$$

where ω_{*N} and ω_{*T} are the diamagnetic drift frequencies due to particle density and temperature gradients, respectively. For simplicity, we take an assumption that the equilibrium plasma density is constant, thus $\omega_{*N} = 0$. ω_E is the $\mathbf{E}\times\mathbf{B}$ rotation frequency, again assumed to be a constant:$\omega_E = \omega_0$. $\omega_d = C_d\hat{\varepsilon}_k\lambda[(2E-K)/(2K)]$ is the bounce-averaged toroidal precession frequency of trapped thermal particles due to ∇B drift, with $C_d \equiv \sigma_1 q(\rho_l/r)(\upsilon_{th}/R_0)$ and $\rho_l \equiv \upsilon_{th}/\omega_c$ being the Larmor radius of particle gyro-motion, with the gyro-frequency $\omega_c = eB_0/M$. $\upsilon_{th} \equiv \sqrt{2T/M}$ is the thermal speed of the particle with mass M. $\sigma_1 = +1$ for ions and $\sigma_1 = -1$ for electrons. E is the complete elliptic integral of the second kind.

One key element of the present study is to investigate how the plasma collisionality can affect the drift kinetic damping and eventually on the mode dynamics. In a previous work [14], it has been shown that the collisionality can sensitively change the drift kinetic damping on the RWM. In this work, we discover another important role played by the particle collisions, namely the triggering of the bifurcation in the mode dynamics. The effective collisionality is denoted by ν_{eff} in the resonance operator (5). We consider two collision models: the energy-independent model $\nu_{eff} = \nu \equiv \frac{\sqrt{2}n_i m_{ij}^{1/2} Z_i^2 Z_j^2 e^4}{12\pi^{3/2}\epsilon_0^2 m_j T_j^{3/2}}\ln\Lambda$, and a model where the effective collision frequency is also a function of the particle energy $\nu_{eff} = \nu\hat{\varepsilon}_k^{-3/2}/\epsilon_r$, on top of the neoclassical correction. Here $m_{ij} = m_i m_j/(m_i + m_j)$, Z the particle charge number, $\ln\Lambda$ the Coulomb logarithm, and ϵ_0 the vacuum permittivity. In this work, we assume that for thermal ions, the ν value, when normalized by the Alfvén frequency, varies in the range of $10^{-5} \sim 10^{-3}$. The collisionality for thermal electrons is $(2m_i/m_e)^{1/2}$ times larger than that for thermal ions.

Using the $m/n = 2/1$ eigen-function of the RWM for a circular cylindrical equilibrium the drift kinetic energy perturbation (2) is analytically derived as

$$\delta W_k = \frac{\mu_0^2 J_0^2}{\pi^{1/2}B_0^2}\sum_{e,i}\int_0^1 dr r^{2(u-1)}(1-r^2) \times \int_{\frac{1}{1+\epsilon_r}}^{\frac{1}{1-\epsilon_r}} d\lambda[G_0^2 + 4k_t^2 G_1^2]\frac{K(2-\lambda)^2}{\sqrt{2\lambda\epsilon_r}}\int_0^\infty d\hat{\varepsilon}_k[\Omega_b\hat{\varepsilon}_k + \Omega_n\Omega_b + \Omega_b(\frac{\Omega_a+\Omega_n}{\Omega_b} - \Omega_n)]\frac{\hat{\varepsilon}_k^{5/2}e^{-\hat{\varepsilon}_k}}{\hat{\varepsilon}_k D + \Omega_n}, \qquad (6)$$

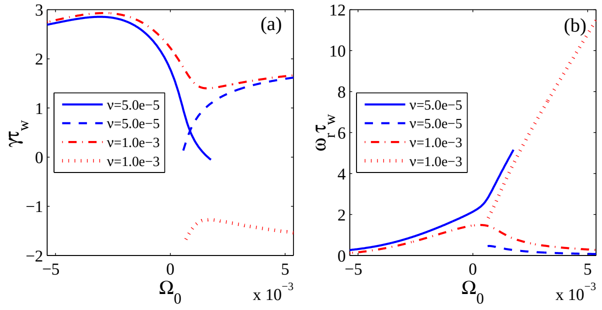

FIG. 1. (color online). The (a) real, and (b) imaginary, parts of the n=1 RWM eigenvalue, normalized by the wall time τ_w, versus the toroidal $\mathbf{E}\times\mathbf{B}$ rotation frequency. Compared are two cases with low and high thermal ion collisions, with each case having two branches of the RWM as predicted by the analytic model. Both the $\mathbf{E}\times\mathbf{B}$ rotation frequency and the collision frequency are normalized by the Alfvén frequency.

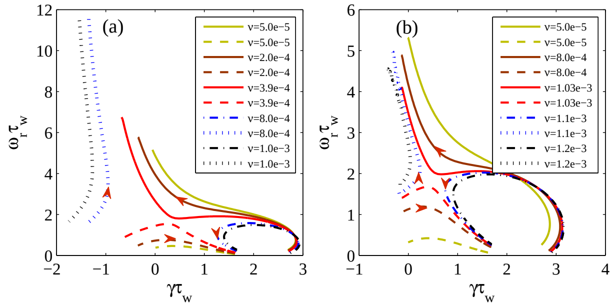

FIG. 2. (color online). The real (γ) and imaginary (ω) parts of the n=1 RWM eigenvalue normalized by the wall time τ_w, as predicted by the analytic model with various values of the collisionfrequency. Considered are (a) a simple Krook collision model with effective collision frequency $\nu_{eff}=\nu$ for thermal ions, and (b) a collision model with particle energy dependence as well as the neoclassical correction $\nu_{eff}=\nu\hat{\varepsilon}_k^{-3/2}/\epsilon_r$. Arrows along the curves indicate the direction of increasing the toroidal flow velocity.

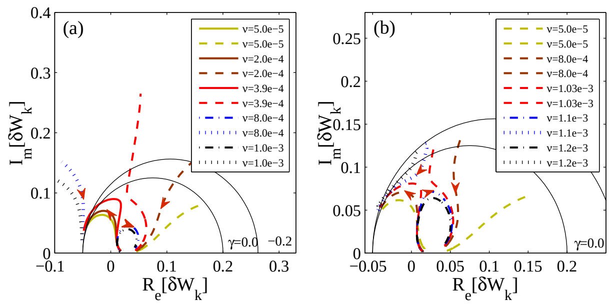

FIG. 3. (color online). The perturbed drift kinetic energy, plotted in the complex plane, calculated for the same cases (a) and (b) as in Fig.2. Circles indicate constant values for the growth/damping rate of the mode.

where $D=\lambda(E/K-1/2)$, and we have introduced the following factors

$$\Omega_a=\frac{n\omega_{*N}-3n\omega_{*T}/2+i\nu_{eff}}{nC_d},\Omega_b=\frac{n\omega_{*T}}{nC_d},$$

$$\Omega_n=\frac{n\omega_E-\omega-i\nu_{eff}}{nC_d}.$$

In further study, we numerically solve the non-linear dispersion relation (1) for a fixed equilibrium with $a=1m$, $R_0=3m$, $B_0=3T$, $q_0=1.42$. A resistive wall with thickness $d=0.01a$ is located at $b=1.20a$. The $m/n=2/1$ mode is considered. Whilst the drift kinetic energy (6) is exactly evaluated following these conditions, we choose the values for the fluid potential energies such that (i) the (fluid) RWM is unstable without the drift kinetic damping, and (ii) the fluid potential energy is by magnitude comparable to the drift kinetic energy. This is often the case from the results of the self-consistent toroidal computations (which is also why the drift kinetic terms can strongly affect the RWM stability). Here we set $\delta W_b=0.05$ and $\gamma_f\tau_w=-\delta W_\infty/\delta W_b=4$. We find qualitatively the same results while varying these fluid parameters within reasonable ranges.

Figure 1 compares the solution of the dispersion relation (1) at two extreme values of the thermal ion collision frequency, $\nu=5.0\times10^{-5}$ and $\nu=1.0\times10^{-3}$. The simple collision model, without the particle energy dependence, is assumed here. In both high and low collisionality regimes, there are two branches of the RWM. However, these two branches behave qualitatively differently as the $\mathbf{E}\times\mathbf{B}$ flow velocity varies. With increasing collision frequency, these two branches merge and form two new branches. This transition is more clearly shown in Fig. 2(a), where we plot the eigenvalue of the mode in complex plane, for various choices of the collision frequency. The arrows along the curves indicate the direction of increasing the $E\times B$ flow velocity. Two separatrix lines exist, that divide the complex plane into four regions. Depending on the particle collision, the modes eigenvalue can only be located in two of the four regions (i.e. either side of the separatrix). This is similar to the bifurcation (of saddle type) of a dynamic system in the phase space. In practice, this result predicts that the behavior of the RWM (both growth rate and mode frequency), with varying plasma flow speed, can be rather different depending on the plasma collisionality regime. More specifically, at low collisionality, the plasma flow induced drift kinetic resonance tends to stabilize one branch of the mode but destabilizes the other one, whilst at high collisionality, increasing of the flow speed does not generally change the stability of either of the branches.

Figure 2(b) shows the same phenomenon, but obtained using the particle energy-dependent collision model. Plotted in the figure are also cases where two unstable branches of the RWM co-exist for the same set of plasma parameter values. The bifurcation of the RWM dynamics is inherently related to the non-linear dependence of the perturbed drift kinetic energy on the mode eigenvalue. Indeed, the bifurcation also occurs when plotting $\mathtt{R_e}(\delta W_k)$ versus $\mathtt{I_m}(\delta W_k)$ in complex plane, as shown in Fig. 3. The circles in these plots indicate constant growth or damping rates of the mode. This can be understood by re-writing the real part of the dispersion relation (1) into the following form

$$(\mathtt{R_e}(\delta W_k) - \Theta)^2 + (\mathtt{I_m}(\delta W_k))^2 = \Gamma^2, \tag{7}$$

$$\Gamma = (\delta W_b - \delta W_\infty)/[2(1 + \mathtt{R_e}(\gamma\tau_w))], \tag{8}$$

$$\Theta = -\frac{(\delta W_b + \delta W_\infty)}{2} - \frac{(\delta W_b - \delta W_\infty)\mathtt{R_e}(\gamma\tau_w)}{2[(1 + \mathtt{R_e}(\gamma\tau_w)]}. \tag{9}$$

The marginal stability circle is obtained by setting $\mathtt{R_e}(\gamma\tau_w) = 0$ in Eqs. (8, 9). The RWM is stable when $\mathtt{R_e}(\delta W_k)$ and $\mathtt{I_m}(\delta W_k)$ are located outside this circle. It is interesting to note that the point $\mathtt{R_e}(\delta W_k) = -\delta W_b$, $\mathtt{I_m}(\delta W_k) = 0$ always satisfies Eq. (7), independent of the value of $\mathtt{R_e}(\gamma\tau_w)$. Therefore, all the equal-growth/damping rate circles in the complex domain for δW_k crosses this point. Another interesting consequence is that the RWM dispersion relation (1) predicts a full stability of the mode whenever $\mathtt{R_e}(\delta W_k) < -\delta W_b$, independent of the value for $\mathtt{I_m}(\delta W_k)$.

Independent of the sign, the imaginary part of the perturbed drift kinetic energy δW_k always plays a stabilizing role for the mode, as can be qualitatively understood from Fig. 3. However, the real part of δW_k can be either stabilizing or destabilizing. The separatrix lines in the complex plane for δW_k defines the boundaries for these two qualitatively different roles played by $\mathtt{R_e}(\delta W_k)$. At low collisionality, the real part of δW_k is generally stabilizing for one branch of the RWM (the one which is unstable at vanishing flow) but destabilizing for the other branch (which is stable at vanishing flow). At high collisionality, the $\mathtt{R_e}(\delta W_k)$ does not vary much for the unstable branch, having generally low magnitude. This branch thus remains unstable as the flow speed increases. The stable branch at high collisionlity remains stable as flow changes, for the case shown in Fig. 3(a), mainly due to the fact that $\mathtt{R_e}(\delta W_k) < -\delta W_b$. This is, however, not always the case. With the particle energy dependent collisionality model (Fig. 3(b)), the value of $\mathtt{R_e}(\delta W_k)$ varies in such a way, that the marginal stability boundary is crossed twice as the flow speed increases.

A more qualitative understanding can be gained by studying the instability condition for RWM, derived again from the dispersion relation (1) [11, 20]

$$-\delta W_b \delta W_\infty > |\delta W_k|^2 + \mathtt{R_e}(\delta W_k)(\delta W_b + \delta W_\infty). \tag{10}$$

In this work, since we choose $\delta W_b + \delta W_\infty < 0$, a negative (positive)value of $\mathtt{R_e}(\delta W_k)$ is stabilizing (destabilizing). This is clearly demonstrated in Fig. 4(a), where

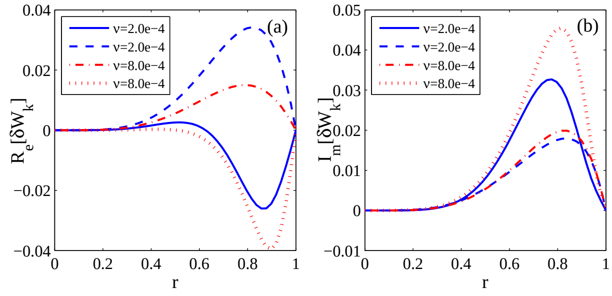

FIG. 4. (color online). Radial profiles for (a) real and (b) imaginary parts of the perturbed drift kinetic energy, calculated for two (thermal ion) collision frequencies. Compared are also δW_k for two branches of the mode at each frequency. Shown are cases with energy independent collision model, at $E \times B$ rotation frequency $\omega_0/\omega_A = 0.001$.

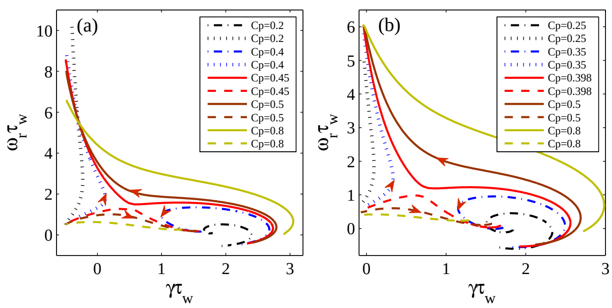

FIG. 5. (color online). The real (γ) and imaginary (ω) parts of the n=1 RWM eigenvalue normalized by the wall time τ_w, as predicted by the analytic model with a fixed collision frequency $\nu = 2.0 \times 10^{-4}$ and with varying parameter C_p. Considered are two collision models, (a) without, and (b) with, the particle energy dependence in the Krook collision operator. Arrows along the curves indicate the direction of increasing the toroidal flow velocity.

the radial distributions of $\mathtt{R_e}(\delta W_k)$ are compared for two (low and high) collisionality cases, with each case having two branches. The imaginary parts, shown in Fig. 4(b), are always stabilizing.

The thermal particle collisionality is not the only parameter that determines the bifurcation of the RWM dynamics in this analytic model. It turns out that, by varying the thermal ion and electron temperature ratio, similar behavior is found. Defining a parameter $C_p = T_i/(T_e + T_i)$, figures 5(a, b) again plot the eigenvalue of the mode in the complex plane, with different values of C_p. The arrows along the curves again indicate the direction of increasing the plasma $E \times B$ flow speed. The collision frequencies are fixed for both ions and electrons in this scan. The existence of the two separatrix lines are evident, without (a) or with (b) the particle energy dependence in the collision frequency.

The analytic model, presented here by Eqs. (1) and (6), is greatly simplified (cylindrical equilibrium with circu-

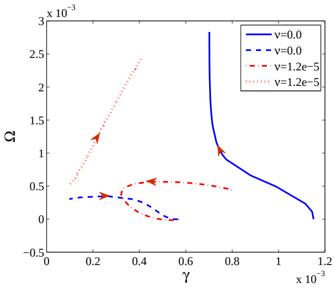

FIG. 6. (color online). The real (γ) and imaginary (ω) parts of the eigenvalue (normalized by the on-axis Alfvén frequency) of the n=1 RWM, computed by the MARS-K code for a full toroidal Solovév equilibrium. Both thermal ion and electron collisions are included, with $\nu_i = \nu$, $\nu_e \approx 86\nu_i$. The equilibrium temperature of ions and electrons are assumed equal ($C_p = 0.5$). Arrows along the curves indicate the direction of increasing the toroidal flow velocity.

lar cross section, constant q-profile, eigenfunction with single poloidal harmonic and with prescribed radial profile). In order to verify whether the bifurcation predicted by this model also occurs in toroidal geometry, we have performed a self-consistent computations of the RWM eigenvalue using the MHD-kinetic hybrid code MARS-K [13], for a toroidal Solovév equilibrium. This equilibrium, also used in a recent extensive codes benchmark efforts [21], has the aspect ratio of 3, the elongation of 1.6 for the poloidal cross section of the plasma, the on-axis safety factor of 1.9, and the normalized beta value of $\beta_N = 2.85$. Kinetic contributions from processional drift resonances of both trapped thermal ions and electros are included in the MARS-K computations. Although computationally much more challenging compared to solving the analytic dispersion relation (1), we find qualitatively similar bifurcation behavior, as shown in Fig. 6.

In summary, based on both an analytic model and the full toroidal computations using the MARS-K code, we have discovered a bifurcation of the RWM dynamics, in the sense that the mode's eigenvalue, as a function of the toroidal flow speed, experiences qualitative change with continuous variation of certain plasma parameters (the particle collision frequencies or the equilibrium thermal ion to electron temperature ratio). Two separatrix lines divide the complex plane of the modes eigenvalue into four regions, where the modes dynamics, as well as the associated drift kinetic energy perturbations, are found to be qualitatively different. This work thus predicts a more complicated behavior than previously thought, of the RWM dynamics due to drift kinetic resonances, depending on the plasma regimes.

This work was supported by National Magnetic Confinement Fusion Science Program (Grant Nos. 2014GB124000, 2013GB111000 and 2013GB112009) and by National Natural Science Foundation of China (NSFC) [Grant Nos.11428512, 11322549, 11205051 and 11475056]. Work is also partially funded by the European Union's Horizon 2020 research and innovation programme under grant agreement number 633053 and from the RCUK Energy Programme [grant number EP/I501045]. The views and opinions expressed herein do not necessarily reflect those of the European Commission.

* haogz@swip.ac.cn
† zxwang@dlut.edu.cn

[1] T. C. Hender *et al.*, Nucl. Fusion **47**, S128 (2007).
[2] M. S. Chu and M. Okabayashi, Plasmas Phys. Controlled Fusion **52**, 123001 (2010).
[3] D. Gregoratto *et al.*, Phys. Plasmas **12**, 092510 (2005).
[4] Z. R. Wang *et al.*, Phys. Rev. Lett. **114**, 145005 (2015).
[5] S. A. Sabbagh *et al.*, Nucl. Fusion **46**, 635 (2006).
[6] M. P. Gryaznevich *et al.*, Plasma Phys. Controlled Fusion **50**, 124030 (2008).
[7] H. Reimerdes *et al.*, Phys. Rev. Lett. **98**, 055001 (2007).
[8] M. Takechi *et al.*, Phys. Rev. Lett. **98**, 055002 (2007).
[9] A. Bondeson and D. J. Ward, Phys. Rev. Lett. **72**, 2709 (1994).
[10] Y. Q. Liu and A. Bondeson, Phys. Rev. Lett. **84**, 907 (2000).
[11] B. Hu and R. Betti, Phys. Rev. Lett. **93**, 105002 (2004).
[12] I. T. Chapman *et al.*, Plasma Phys. Controlled Fusion **51**, 055015 (2009).
[13] Y. Q. Liu *et al.*, Phys. Plasmas **16**, 056113 (2009).
[14] J. W. Berkery *et al.*, Phys. Rev. Lett. **106**, 075004 (2011).
[15] G. Z. Hao *et al.*, Phys. Rev. Lett. **107**, 015001 (2011).
[16] Y. L. He *et al.*, Phys. Rev. Lett. **113**, 175001 (2014).
[17] Y. Q. Liu *et al.*, Phys. Plasmas **15**, 092505 (2008).
[18] J. W. Berkery, R. Betti and S. A. Sabbagh, Phys. Plasmas **18**, 072501 (2011).
[19] Y. Q. Liu *et al.*, Phys. Plasmas **15**, 112503 (2008).
[20] G. Z. Hao *et al.*, Phys. Plasmas **19**, 032507 (2012).
[21] J. W. Berkery *et al.*, Phys. Plasmas **21**, 052505 (2014).